

New Scheme for Positron Accumulation in Ultrahigh Vacuum

N. Oshima,^{1,2} T. M. Kojima,² M. Niigaki,^{1,2} A. Mohri,² K. Komaki,¹ and Y. Yamazaki^{1,2}

¹*Institute of Physics, University of Tokyo, 3-8-1 Komaba, Meguro, Tokyo 153-8902, Japan*

²*Atomic Physics Laboratory, RIKEN, 2-1 Hirosawa, Wako, Saitama 351-0198, Japan*

(Received 9 March 2004; published 4 November 2004)

A new positron accumulation scheme compatible with ultrahigh vacuum conditions has been developed, which is realized by preparing a high density electron plasma as high as $\approx 10^{11} \text{ cm}^{-3}$ and an ion cloud as energy absorbers. The present accumulation rate normalized by the intensity of ^{22}Na positron source is $(3.6 \pm 0.3) \times 10^2 e^+/\text{s/mCi}$, which is more than one and a half orders of magnitude higher than other ultrahigh vacuum compatible schemes so far reported.

DOI: 10.1103/PhysRevLett.93.195001

PACS numbers: 52.40.Mj, 52.27.Ep, 52.27.Jt

Positron accumulation schemes have been intensively studied in the last two decades [1–7], and can be applied to various fields of science such as low energy collision experiments with gases [8] and possibly with surfaces [9], plasma physics [10], antihydrogen synthesis [11], positronium production [12,13], and positron cooling of highly charged ions [14]. These subjects often require an ultrahigh vacuum (*UHV*) environment, and, hence, to realize a high-efficiency positron accumulation under *UHV* conditions is one of the key issues of the field.

UHV compatible schemes to accumulate positrons from ^{22}Na sources so far developed are resistive cooling [2] and field ionization of positronium in high Rydberg state [3], the accumulation rates of which were $\approx 3.3 \times 10^{-2}$ and $\approx 1.1 \times 10^1 e^+/\text{s/mCi}$, respectively. The rate was normalized by the ^{22}Na source intensity. A magnetic bottle scheme [6,12] and a stochastic transport in a Penning trap [7] were also studied, which had only a short confinement time. When *UHV* requirements are relaxed, an N_2 buffer gas method is proved to be quite efficient, more than $10^4 e^+/\text{s/mCi}$ [1], where positrons are accumulated in vacuum of $\sim 10^{-4}$ Pa. In this case, the maximum accumulation time is ≈ 100 seconds (s) due to annihilation of positrons with the buffer gas. This Letter reports a conceptually new scheme of positron accumulation, which is proved to be at least one and a half orders of magnitude more efficient than other *UHV* compatible schemes above and has no limit on the accumulation time. The key ingredient of the present scheme is a combination of a high density electron plasma ($\approx 10^{11} \text{ cm}^{-3}$) [15] and an ion cloud. In the case of antihydrogen synthesis, for example, the present scheme provides a large number of trapped positrons next to the antihydrogen recombination trap in the *UHV* environment, which allows access to and extraction of antihydrogen atoms in the recombination trap (see, e.g., Ref. [16]).

Figure 1(a) shows a schematic configuration of the experimental setup [17], which consists of an electron gun (EG), a multiring trap (MRT) [18], a movable remoderator (RM), a Faraday cup (FC), and a NaI γ -ray detector. The MRT and RM are in a cryogenic

UHV bore tube of a 5T superconducting (SC) solenoid. The MRT was adopted because it can flexibly prepare various harmonic wells, where a large number of positively and/or negatively charged particles are stably confined simultaneously. The positron accumulation proceeds according to the following processes: (1) preparation of electron and ion clouds in the MRT, (2) injection of positrons on the RM along the axis of the MRT, (3) slowing down of reemitted positrons from the RM through interaction with the electron cloud, (4) accumulation of positrons assisted by the ion cloud, and (5) self-cooling of positrons through synchrotron radiation.

The MRT used in the present experiment consists of 21 equally spaced cylindrical electrodes, each 2.3 cm in length, sandwiched between two 16 cm long cylindrical

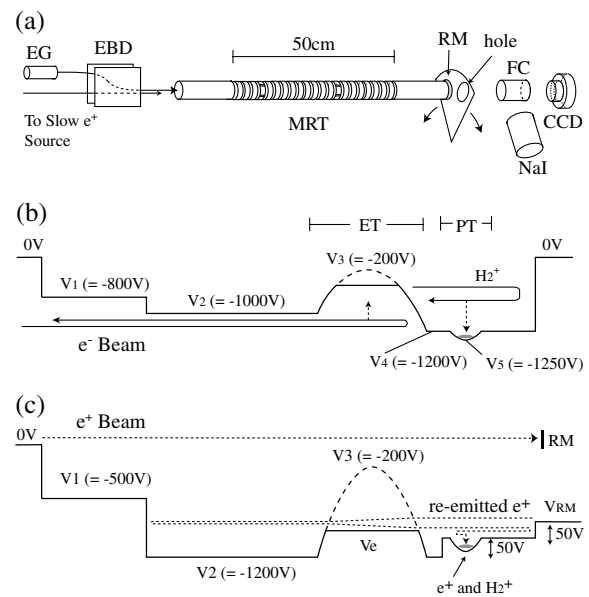


FIG. 1. (a) A schematic diagram of the experimental setup consisting of an electron gun (EG), a multiring trap (MRT), a movable remoderator (RM), a Faraday cup (FC), and a NaI detector. (b) The electric potential configuration along the MRT axis in the electron-ion accumulation mode. (c) The same as (b) in the positron accumulation mode (see text).

electrodes on both ends. All the trap electrodes have the same inner diameter of 3.8 cm. The bore tube was cooled down to 10 K, which was essential to maintain *UHV* environment around the MRT. The EG is installed at ≈ 110 cm upstream of the MRT and 2.5 cm off the MRT axis. The RM was mounted on a movable arm at the downstream end of the MRT. The FC was placed at ≈ 60 cm downstream from the end of the MRT to measure the total charge of the electron cloud. The end cap of the FC is made of aluminum coated phosphor on an Indium-Tin-Oxide glass plate to observe the radial distribution of the electron cloud with the charge coupled device (CCD) camera (see Fig. 1(a)). The magnetic field at the FC was $\approx 1/100$ of that around the center of the SC solenoid; i.e., the diameter of the image on the phosphor screen is ≈ 10 times larger than the diameter of the electron cloud in the MRT. The NaI scintillator was used to detect γ -rays from annihilation of positrons arriving at the FC. Its detection efficiency was calibrated by inserting a standard source of ^{22}Na at the FC. The source had 3% uncertainty in its intensity, which determined the systematic error of the positron intensity at the FC.

Figure 1(b) shows the electric potential configuration along the MRT axis when the system was operated under an electron-ion accumulation mode. The MRT electrodes were biased so that two harmonic potentials were formed; one was ≈ 35 cm long for electrons [electron trap (ET)] and the other ≈ 12 cm long for positrons and ions [positron trap (PT)]. The potential depths of the ET and PT were set to 1 kV and 50 V, respectively. An electron beam of 1040 eV from the EG was guided on the axis of the MRT across the magnetic field with the $\mathbf{E} \times \mathbf{B}$ deflector (EBD), introduced in the MRT, and reflected back at the downstream barrier of the ET. The electron beam current was typically $\approx 1 \mu\text{A}$. The number of electrons accumulated in the ET, N_e , was controlled by varying the injection time (10-40 s) with its fluctuation less than $\approx 5\%$ [17]. The intensity distribution of the CCD image provides the electron column density $n_e l$, where n_e is the electron density and l is the axial length of the electron cloud. In the present experiment, $n_e l$ was reasonably represented by $\alpha(N_e) \exp(-r^2/r_e^2)$ near the center of the MRT axis, where r_e was around $\approx 3 \times 10^{-2}$ cm weakly depending on N_e in the present experiment. The electrons in the MRT cool themselves via synchrotron radiation down to the environmental temperature with a cooling time of $\sim 6B[\text{T}]^{-2}$ s [19] and actually behave as a non-neutral plasma because the Debye length is much shorter than r_e .

Positive ions were produced in and upstream of the ET via ionization of residual gases during injection of the electron beam. The ion species in the PT was identified to be H_2^+ by monitoring the longitudinal oscillation excited by a pulsed rf field. The total number of ions was typically $\sim 1 \times 10^8$ for electron injection of 30 s, which is consistent with the number of ionized atoms calculated, taking

into account the partial pressure of H_2 around the MRT and the electron beam current [20]. The accumulation of H_2^+ ions in the PT would be enhanced via resonant charge transfer processes between H_2^+ ions formed upstream of the PT and H_2 molecules in the residual gas around the PT [21], which would produce thermal H_2^+ ions in the PT and fast H_2 molecules.

Figure 1(c) shows the electric potential configuration along the MRT axis for the positron accumulation mode. The positron source was located ≈ 4 m upstream of the SC solenoid, which consists of a ^{22}Na (22 mCi) β^+ emitter and a solid Ne moderator [22]. Slow positrons of $\approx 1.6 \times 10^6 e^+/\text{s}$ were generated and transported to the SC solenoid with a set of guiding coils and two sets of steerers. The radius of the positron beam in the SC solenoid is estimated to be $r_p \approx 2.5 \times 10^{-2}$ cm because the Ne moderator of ≈ 0.8 cm in diameter was in a magnetic field of ≈ 0.02 T. A magnetic mirror formed near the entrance of the SC solenoid limited the transmission efficiency to be $\approx 50\%$ and caused longitudinal energy spreads of more than several hundred eV in the solenoid. To realize efficient accumulation, this large energy spread was compressed by injecting positrons in the RM, from which positrons were reemitted with kinetic energies $E_{\text{RM}} \leq 3$ eV [23].

The reemitted positrons make a round trip reflected at the potential wall V_1 toward the RM, passing the electron plasma and the ion cloud 2 times. During the round trip, positrons lose their kinetic energies via collisions with electrons in the ET. When the electron column density is high enough so that the longitudinal energy loss is larger than E_{RM} during the round trip, the positrons do not reach the RM and oscillate between the RM and the potential wall V_1 . During the oscillation, the positrons suffer elastic and inelastic collisions with H_2^+ ions in the PT, resulting in further longitudinal energy reduction, and are eventually accumulated in the PT. Positrons in the PT cool themselves via synchrotron radiation like in the case of electrons.

The injection energy of the reemitted positrons to the electron plasma E_i was adjusted by varying the RM bias V_{RM} . The solid circles and solid triangles in Fig. 2 show the accumulation efficiencies ε_a of positrons in the PT as a function of V_{RM} for $N_e \approx 1.8 \times 10^{10}$ and 1.2×10^{10} , respectively. Here, ε_a is the ratio of the number of positrons accumulated in the PT to the number of positrons injected in the RM. The behavior of ε_a is qualitatively understood in the following way: (1) When V_{RM} is lower than the electron plasma potential V_e (see Fig. 1(c)), the reemitted positrons are reflected back in front of the plasma and, hence, ε_a is almost zero. (2) On the other hand, when $V_{\text{RM}} \gg V_e$, all the reemitted positrons penetrate through the plasma but the energy loss is relatively small, and, hence, ε_a is again small. (3) When V_{RM} is adjusted to $\approx V_e$, a considerable fraction of reemitted positrons can penetrate into the plasma with relatively low energy, resulting in sufficient energy loss and accordingly large

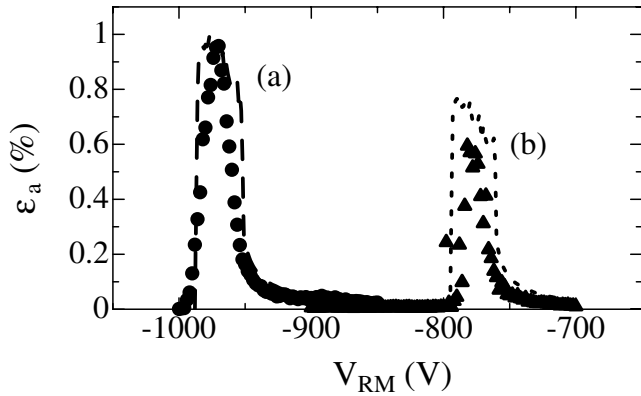


FIG. 2. The accumulation efficiency ϵ_a of positrons in the PT as a function of the remoderator bias V_{RM} for (a) $N_e \approx 1.8 \times 10^{10}$ and (b) 1.2×10^{10} . Here, ϵ_a is defined as the ratio of the number of positrons accumulated in the PT to the number of positrons injected in the RM during accumulation.

ϵ_a . Figure 2 shows that the maximum accumulation efficiency ϵ_a^{\max} was as high as $\approx 1\%$ at $V_{RM}^{\max} \approx 970$ V for $N_e \approx 1.8 \times 10^{10}$.

Figures 3(a) and 3(b) show ϵ_a^{\max} and V_{RM}^{\max} as a function of N_e . It is seen that ϵ_a^{\max} increases monotonically with N_e . The right vertical scale gives the accumulation rate normalized by the ^{22}Na source intensity. The accumulation rate achieved in the present scheme was $\approx 360 e^+/\text{s/mCi}$, which was more than 30 times higher than those of other *UHV* compatible techniques so far reported [2,3]. This high rate stayed constant for about 100 s and then slowly lowered due primarily to the radial expansion of the electron plasma. By reloading electron

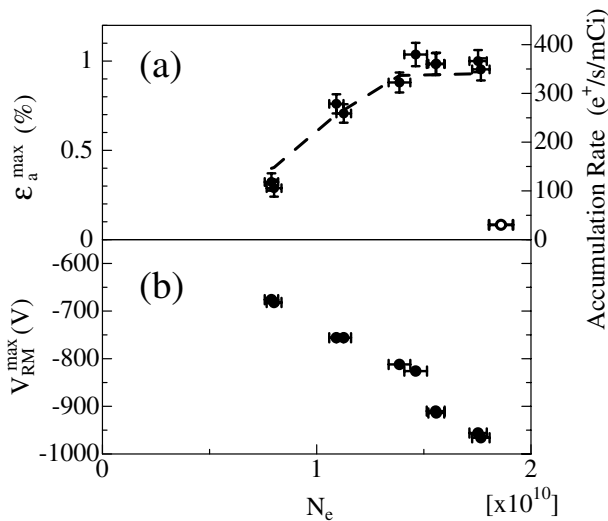


FIG. 3. (a) The optimized accumulation efficiency ϵ_a^{\max} and (b) the corresponding remoderator bias V_{RM}^{\max} as a function of N_e . The right vertical scale of the panel (a) gives the accumulation rate normalized by the ^{22}Na positron source intensity. The vertical error bars reflect statistical errors, which do not include the systematic error of 3%. The horizontal error bars show reproducibility of N_e .

plasmas every 100 s, which took ≈ 40 s, the above accumulation rate recovered repeatedly for more than 1000 s without noticeable loss of positrons.

To study the accumulation mechanism, the number of positrons in the PT was measured (1) without ions in the PT but with the same number of electrons in the ET, and (2) without electrons but with ions. In the former case, the accumulation rate was $\approx 0.1\%$ as marked by the open circle at the right lower corner of Fig. 3(a). In other words, ions in the PT enhance the efficiency by a factor of 10 once positrons are slowed down by electrons. In the latter case, no positrons were accumulated because all the reemitted positrons are reflected in front of the ET, which is practically the same condition as that with electrons in the ET but with $V_{RM} \ll V_e$ (see Fig. 2). These observations prove that the positron accumulation is governed by the energy loss of positrons in the electron plasma.

With no electrons in the ET, the electric potential $V_e(r, z)$ is approximately given by $-\beta z^2 - V_3'$ at $r = 0$ like the dashed line in Fig. 1(c) ($\beta \approx 3.8 \text{ V cm}^{-2}$ and $V_3' \approx 209$ V in the present conditions), which is modified like the solid line in Fig. 1(c) when the electron plasma is in the ET. The plasma length corresponds to the length of the flat part. Equating $V_e(0, l/2)$ to the experimentally determined V_{RM}^{\max} , the plasma length l is obtained as a function of N_e . Combining l and the column density $n_e l$ obtained from the CCD image, the electron density at $r \approx 0$ was evaluated to be $0.9 \times 10^{11} \leq n_{e0} \leq 1.6 \times 10^{11} \text{ cm}^{-3}$ in the present experimental conditions. The electric potential in the electron plasma $V_e(r, z)$ is then obtained by [24]

$$V_e(r, z) \equiv V_e(r) \approx V_{RM}^{\max} + \frac{en_e r^2}{4\epsilon_0}, \quad (1)$$

near the axis of the plasma, where e is the electron charge and ϵ_0 is the permittivity of vacuum.

The stopping power of a positron with its kinetic energy E in an electron cloud is approximately given by $\kappa n_e / E$ ($\kappa \approx 1.5 \times 10^{-12} \text{ eV}^2 \text{ cm}^2$) if $E \gg k_B T_e$ [25], where k_B is the Boltzmann constant and T_e the temperature of the electron cloud. When a positron enters the electron plasma at r , its kinetic energy in the plasma is given by $E_i = E_{RM} + e[V_{RM} - V_e(r)]$, where E_{RM} is the kinetic energy of the positron reemitted from the RM. Using the stopping power given above, the energy loss of the positron after the round trip through the electron cloud is approximately given by

$$\begin{aligned} \delta E(r, E_{RM}) &= E_i - (E_i^2 - 4\kappa n_e l)^{1/2} \quad \text{for } E_i^2 > 4\kappa n_e l, \\ &= E_i \quad \text{for } E_i^2 < 4\kappa n_e l. \end{aligned} \quad (2)$$

When $\delta E > E_{RM}$, positrons are confined between the RM and the potential wall V_1 and are eventually accumulated in the PT. On the other hand, if $\delta E < E_{RM}$, positrons are reinjected in the RM and a considerable fraction of them is lost. The overall accumulation efficiency is then given

by

$$\varepsilon_a \approx \frac{\varepsilon_{RM} \int_0^{r_p} \int_0^{E_{max}} 2\pi r f(E_{RM}) p(r, E_{RM}) dE_{RM} dr}{\pi r_p^2 \int_0^{E_{max}} f(E_{RM}) dE_{RM}}, \quad (3)$$

where $f(E_{RM})$ is the energy distribution of reemitted positrons, E_{max} is the maximum positron energy emitted from the RM, which is ≈ 3 eV, and $p(r, E_{RM})$ is the trapping probability of a positron. To simplify the situation, we put the trapping probability $p(r, E_{RM})$ to be one (0) if $\delta E > E_{RM}$ ($\delta E < E_{RM}$). Assuming $f(E_{RM})$ is approximated by $\exp[-(\frac{E_{RM}-\bar{E}_{RM}}{\Delta E})^2] + C$, the parameters (\bar{E}_{RM} , ΔE , C , and ε_{RM}) are determined so that ε_a in Fig. 2 and ε_a^{max} in Fig. 3(a) are reproduced. The dashed and dotted lines in Fig. 2 and dashed line in Fig. 3(a) are the results of the best fit, where \bar{E}_{RM} , ΔE , C and ε_{RM} were 2.9 eV, 0.2 eV, 0.01 and 0.13, respectively. These values are consistent with known values [23].

The loss rate of positrons with electrons in the plasma via radiative and three body recombination processes is $\approx 10^{-2} \text{ s}^{-1}$ in the present experimental conditions [26], which is 100 times lower than the cooling time of remoderated positrons via synchrotron radiation [19]. In other words, the positrons are separated from the electron plasma well before the recombination loss gets really serious. The contribution of direct annihilation is even smaller than the above rate [27].

Summarizing, $\approx 1\%$ of positrons injected into the MRT are successfully accumulated under *UHV* condition by combining a high density electron plasma of $n_e \approx 10^{11} \text{ cm}^{-3}$ and an ion cloud. It was found that the energy loss of positrons in the electron plasma plays an essential role and the ion (H_2^+) cloud enhances the positron accumulation rate by an order of magnitude. In spite of a relatively low efficiency of the Ne moderator used here, $\approx 1/3$ of a reported value [22], the accumulation rate normalized by the ^{22}Na source intensity (3.6 ± 0.3) $\times 10^2 \text{ e}^+/\text{s/mCi}$ was at least one and a half orders of magnitude higher than those reported by other *UHV* compatible methods [2,3]. The positron accumulation efficiencies were reasonably reproduced taking into account the energy loss of positrons in a non-neutral electron plasma.

The authors are grateful to H. Higaki, T. Kambara, Y. Kanai, S. Letout, Y. Nakai, H. Oyama, M. Wada, A. Sakai, and R. Suzuki for their vivid discussions and help in developing the experimental setup. This work is supported by Special Research Projects for Basic Science of RIKEN. One of the authors (N.O.) thanks a Special Doctoral Researchers Program in RIKEN and the Japan Society for the Promotion of Science for Young Scientists.

- [1] C. M. Surko *et al.*, Phys. Rev. Lett. **62**, 901 (1989); R. G. Greaves *et al.*, Phys. Plasmas **1**, 1439 (1994).
- [2] L. H. Haarsma *et al.*, Phys. Rev. Lett. **75**, 806 (1995).
- [3] J. Estrada *et al.*, Phys. Rev. Lett. **84**, 859 (2000).
- [4] A. Newbury *et al.*, Phys. Rev. A **62**, 023405 (2000).
- [5] T. Kumita *et al.*, Appl. Surf. Sci. **149**, 106 (1999).
- [6] A. P. Mills, Jr., Appl. Phys. **22**, 273 (1980).
- [7] B. Ghaffari and R. S. Conti, Phys. Rev. Lett. **75**, 3118 (1995).
- [8] S. J. Gilbert *et al.*, Phys. Rev. Lett. **82**, 5032 (1999).
- [9] A. B. Walker *et al.*, Phys. Rev. B **46**, 1687 (1992).
- [10] R. G. Greaves and C. M. Surko, Phys. Rev. Lett. **75**, 3846 (1995); R. G. Greaves and C. M. Surko, Phys. Rev. Lett. **85**, 1883 (2000); B. M. Jelenković *et al.*, Nucl. Instrum. Methods Phys. Res., Sect. B **192**, 117 (2002).
- [11] M. Amoretti *et al.*, Nature (London) **419**, 456 (2002); G. Gabrielse *et al.*, Phys. Rev. Lett. **89**, 213401 (2002).
- [12] S. Chu and A. P. Mills, Jr., Phys. Rev. Lett. **48**, 1333 (1982).
- [13] A. P. Mills, Jr., Nucl. Instrum. Methods Phys. Res., Sect. B **192**, 107 (2002).
- [14] A. Mohri *et al.*, *Non-Neutral Plasma Physics IV*, edited by F. Anderegg *et al.* (Melville, New York, 2002), p. 634; Y. Kanai *et al.*, Phys. Scr., T **92**, 467 (2001).
- [15] The behavior of such a high density plasma is in itself an interesting subject and is being studied.
- [16] A. Mohri and Y. Yamazaki, Europhys. Lett. **63**, 207 (2003).
- [17] N. Oshima *et al.*, Nucl. Instrum. Methods Phys. Res., Sect. B **205**, 178 (2003).
- [18] A. Mohri *et al.*, Jpn. J. Appl. Phys. **37**, 664 (1998); A. Mohri *et al.*, Europhys. Conf. Abstr. **26B** paper 2.033 (2002).
- [19] H. Higaki *et al.*, Phys. Rev. E **65**, 046410 (2002).
- [20] H. Tawara *et al.*, J. Phys. Chem. Ref. Data **19**, 617 (1990).
- [21] H. B. Gilbody and J. B. Hasted, Proc. R. Soc. London A **238**, 334 (1957).
- [22] A. P. Mills, Jr. and E. M. Gullikson, Appl. Phys. Lett. **49**, 1121 (1986); R. G. Greaves and C. M. Surko, Can. J. Phys. **74**, 445 (1996).
- [23] D. M. Chen *et al.*, Phys. Rev. B **31**, 4123 (1985); R. Suzuki *et al.*, Appl. Surf. Sci. **149**, 66 (1999).
- [24] D. H. E. Dubin and T. M. O'Neil, Rev. Mod. Phys. **71**, 87 (1999).
- [25] D. V. Sivukhin, in *Rev. of Plasma Physics*, edited by M. A. Leontovich (Consultants Bureau, New York, 1966), Vol. 4, p.93.
- [26] M. F. Seaton, Mon. Not. R. Astron. Soc. **119**, 81 (1959); M. E. Glinsky and T. M. O'Neil, Phys. Fluids B **3**, 1279 (1991).
- [27] M. Charlton and J. W. Humberston, *Positron Physics*, Cambridge Monographs on Atomic, Molecular and Chemical Physics Vol. 11, (Cambridge University Press, Cambridge, England 2001).